Response Surface Methodology Optimization of Cobalt (II) and Lead (II) Removal from Aqueous Solution Using MWCNT-Fe3O4 Nanocomposite

Goleij, Milad

Department of Chemical Engineering, Shahrood Branch, Islamic Azad University, Shahrood, I.R. IRAN

Fakhraee, Hossein*[+]

Department of Passive Defense Research Group, Logistics and Crisis Management, Malek Ashtar University of Technology, Tehran, I.R. IRAN

ABSTRACT: *The present investigation describes the evaluation of feasibility of MWCNT-Fe_3O_4 nanocomposite toward adsorptive removal of Co(II) and Pb(II) from aqueous solution in batch mode. The Fe_3O_4–MWCNT hybrid was prepared using a simple one-pot strategy via in situ growth of Fe_3O_4 magnetic nanoparticles onto the surface of the MWCNTs. The Fe_3O_4–MWCNT hybrid was characterized by X-ray diffractometry and Field Emission Scanning Electron Microscopy (FESEM). A Response Surface Methodology (RSM) with a Central Composite Design (CCD) was employed to evaluate the effects of solution pH, contact time, temperature, initial heavy metal concentration and adsorbent dosage on the removal efficiency of the heavy metals. Results of analysis of variance (ANOVA) showed that the initial metal concentration and absorbent dosage and their interaction effect were the most significant parameters for Co(II) ion removal. Adsorbent dosage, pH and initial metal concentration had significant influences on the removal efficiency of Pb(II) ions. The optimum pH, time, temperature, initial concentration of metals and adsorbent dosage were found to be 6.5,25 min, 40 °C, 35 mg/L, and 48.3 mg/50mL, respectively. Maximum removal of Pb(II) and Co(II) in optimum condition was 90.2 and 79.34% respectively. Results indicated that nanocomposite can be used as an effective adsorbent for effluent decontamination especially in Pb–Co bearing wastewaters. The equilibrium data were well fitted by the Langmuir model. The removal mechanism of metal ions followed adsorption and ion exchange processes.*

KEYWORDS: *Nanocomposite; Removal; Cobalt; Lead; RSM.*

INTRODUCTION

Because access to safe drinking water is the key to protect public health, clean water has become a basic need of all properly functioning societies. Despite their presence at low concentration ranges, environmental

***** *To whom correspondence should be addressed.*

+ E-mail: fakhraee@iust.ac.ir

1021-9986/2017/5/129-141 *13/$/6.30*

pollutants possess serious threats to freshwater supply, living organisms, and public health.

Contamination of water with toxic metal ions (Hg(II), Pb(II), Cr(III), Cr(VI), Ni(II), Co(II),Cu(II), Cd(II), Ag(I), As(V) and As(III)) is becoming a severe environmental and public health problem. In order to achieve environmental detoxification, various techniques like adsorption, precipitation, ion exchange, reverse osmosis, electrochemical treatments, membrane filtration, evaporation, flotation, oxidation and biosorption processes are extensively used [1-3]. Among these, adsorption is a conventional but efficient technique to remove toxic metal ions and bacterial pathogens from water [4-6].

Development of novel and cost-effective nanomaterials for environmental remediation, pollution detection and other applications has attracted considerable attention. Recent advances suggest that many of the issues involving water quality could be resolved or greatly ameliorated using nanoparticles, nanofiltration or other products resulting from the development of nanotechnology [7-11]

For adsorption of heavy metals from aqueous systems, the most widely studied nanosized metal oxides include iron oxides, manganese oxides, aluminum oxides, and titanium oxides. They are present in different forms, such as particles, tubes and others[12]. The size and shape of NMOs are both important factors to affect their adsorption performance. Efficient synthetic methods to obtain shape-controlled, highly stable, and monodisperse metal oxide nanomaterials have been widely studied during the last decade[13] .

The facileness of resource and ease in synthesis render nanosized ferric oxides (NFeOs) to be low-cost adsorbents for toxic metal sorption. Since elemental iron is environmentally friendly, NFeOs can be pumped directly to contaminated sites with negligible risks of secondary contamination [12]. The intensively studied NFeOs for heavy metals removal from water/wastewater include goethite (α-FeOOH), hematite (α -Fe_2O_3) [14-16].

Carbon nanotube CNTs (one of nanosorbents) which have been used for removal of impurities have received special attention for their excellent capabilities of removing heavy metals contaminants from water. The ability of CNTs to adsorb heavy metals is reviewed by many researchers [17] such as Cd^{2+}, Cr^{3+}, Pb^{2+} and Zn^{2+} and metalloids such as arsenic (As) compounds. Composites of CNTs with Fe and cerium oxide (CeO_2) have also been reported to remove heavy metal ions in few studies [18-21] . The defect functionalization of CNTs is based on the conversion of carboxylic groups and other oxygenated sites formed through oxidative purification. The carboxylic groups at the end of the CNTs can be coupled with other functional groups. The oxidized CNTs usually react with thionyl chloride to activate the carboxylic group for a later reaction with amines or alcohols [22].

Response Surface Methodology (RSM) is a collection of mathematical and statistical techniques useful for analyzing the effects of several independent variables on the response. RSM has a important application in the process design and optimization, as well as in the improvement of the existing design. The RSM provides functions and data types for the coding and decoding of factor levels. Appropriate coding is an important element of response-surface analysis. There are good commercial software available to help in designing and analyzing response surface experiments.

In the present work, MWCNT–Fe3O4 nanocomposite powder has been synthesized by in-situ method. The efficiency of prepared nanocomposite for Pb^{2+} and Co^{2+} ions removal from aqueous solution is investigated. Several parameters like the ions concentration , sorbent contact time, initial concentration, pH and adsorbent dosage are examined in order to evaluate a reasonable optimization for the sorption efficiency. Using a Central Composite Designs (CCD), statistically designed experiments were used to determine variables that affect the heavy metal removal efficiency more significantly. Attempts have also been made to optimize the removal process by using response surface optimization techniques.

EXPERIMENTAL SECTION

Materials

Multi-walled carbon nanotubes (purity N95%) were purchased from the Iranian Research Nanomaterials, Inc. Ferric chloride ($FeCl_3{\cdot}6H_2O$), Ferrous chloride ($FeCl_2$ $4H_2O$) were purchased from Sigma-Aldrich Chemicals, USA. All other reagents and solvents were purchased from Aldrich or Merck and used without further purification.

Cobalt and Lead solutions were prepared according to Standard Methods. Stock solutions of Co^{2+} and Pb^{2+}

were prepared by dissolving $Co(NO_3)_2$ and $Pb(NO_3)_2$ in distilled water , respectively. $Co(NO_3)_2$ and $Pb(NO_3)_2$ were of analytical grade and supplied by Merck company (Germany).

Surface modification of MWCNT

The carboxylated MWCNTs (MWCNTs–COOH) were prepared by refluxing the MWCNTs in a mixture of concentrated sulfuric acid and nitric acid (3:1 v/v ratio) at 70 °C for 10 h. After cooling to room temperature the mixture was filtered and washed with double distilled water until the pH of the filtrate became ~7 and finally dried at 80 °C overnight.

Synthesis of MWCNT– Fe3O4 nanocomposite

About 0.4 g of MWCNTs–COOH was dissolved in 70 mL of water by ultrasonic irradiation for 20 min. The mixture was further stirred vigorously for 30 min at 60 °C. Then 177 mg of $FeCl^{3+}/FeCl^{2+}$ salts in the mass ratio of 2:1 was added under stirring. The mixture was stirred vigorously for 30 min under N_2 atmosphere. At last 30 mL of 6% NH4OH aqueous solution was added into the mixture drop by drop at 60 °C during 1 h and reacted for another 2 h. N_2 atmosphere was used during the reaction to prevent critical oxidation. The reaction mixture was then centrifuged, washed with double distilled water and dried. The obtained black precipitate was Fe_3O_4/MWCNT nanoparticles and was ready for use.

The characterization and surface morphology of dried nanocomposite powder were studied by using XRD and Field-emission scanning electron microscopy FESEM measurements. The XRD patterns of the as-prepared products were measured using an XD-3 X-ray diffractometer (PuXi, Beijing, China) with nickel filtered Cu Kα radiation (λ= 0.15406 nm) at a current of 20 mA and a voltage of 36 kV. The scanning rate was 4^o min^{-1} in the angular range of 5–80^o (2θ). Field-emission scanning electron microscopy (FE-SEM) S-4160 Hitachi (Japan) and atomic force microscopy (AFM) Nanos Bruker (Germany) were used to investigate the morphology and size distribution of the prepared nanoparticles.

Batch adsorption experiments:

Design of experiments Response surface methodology (RSM) was used to evaluate the effects of different operating parameters on the removal efficiency of Pb^{2+}, Co(II) ions. It not only shows the optimum conditions, but it also proposes fitted regression models. A 5-level, 5-factor Central Composite Designs (CCD) was used to evaluate the effect of the selected factors on removal efficiency. The four parameters affecting heavy metal removal, namely solution pH (A), contact time (B), adsorbent dosage (C) , initial contaminant concentration (D) and temperature (E) were selected as independent variables, and the removal efficiencies (Y) of Pb(II) and Co(II) were considered as the dependent variables (responses). Variables were coded in accordance with the following equation:

The removal efficiency was calculated as:

$$\%\ \mathrm{Removal} = \frac{(C_i - C_f)}{C_i} \times 100 \qquad (1)$$

Where C_i is the initial concentration (mg/L) and C_f is the final concentration (mg/L).

The experimental range and levels of independent variables for metal ion removal were given in Table 1. A set of 32 experimental runs, including duplicates were designed using CCD. The experimental results were analyzed using Design Expert 8.0 and a regression quadratic polynomial model was proposed as follows:

$$Y(\%) = \alpha_0 + \sum \alpha_i X_i + \sum \alpha_i X_i^2 + \sum \alpha_{ij} X_i X_j + \varepsilon \qquad (2)$$

Where, α_0 is the constant coefficient, α_i, α_{ii} and α_{ij} are the regression coefficient and X_i, X_j indicate t he independent variables. ε represents the random error.

Analyses

Atomic absorption spectrophotometry was used for the analysis of heavy metals in solution.

RESULTS AND DISCUSSION

Adsorbent Characterization

The synthesized MWCNT–Fe3O4 nanocomposite was characterized by powder X-ray diffractometer RD and Field-emission scanning electron microscopy. The MWCNT–Fe3O4 nanocomposite XRD pattern was shown in Fig. 1. The diffraction peak, 2θ is equal to 26° that could be (0 0 2) reflected to MWCNT, similarly the diffraction peak, 2θ is equal to 33.5° that could be (3 1 1) reflected to magnetite (Fe3O4) nanoparticles. The analysis shows, the final samples consist of two phases such as cubic Fe3O4 and MWCNT. No obvious peaks

Table 1: Actual and coded values of the test variables (Alpha=2).

Name	Units	-1 Level	+1 Level	-alpha	+alpha
pH		5	7	4	8
t	min	15	35	5	45
D	mg/50ml	30	60	15	75
C0	ppm	40	80	20	100
T	C	30	50	20	60

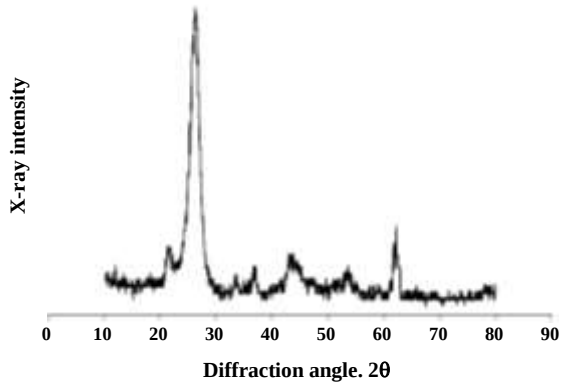

Fig. 1: XRD pattern of MWCNT, Fe3O4 and MWCNT–Fe_3O_4 nanocomposite.

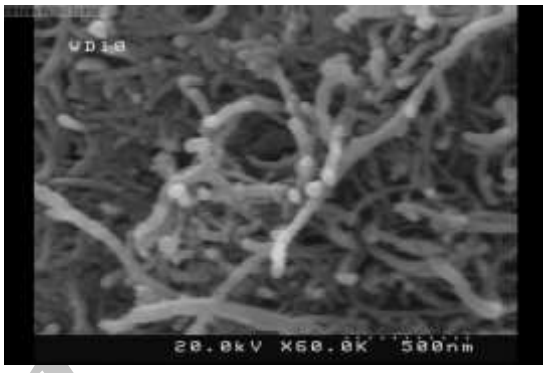

Fig. 2: FESEM results of MWCNT–Fe3O4 nanocomposite.

from other phases were observed. The average size of Fe_3O_4 crystalline calculated using the Scherrer's formula was found as 30 nm.

The FESEM results for synthesized MWCNT–Fe_3O_4 nanocomposite is shown in Fig. 2. It is observed that, the shape of the particles is in cubic shape and also clearly indicates that Fe3O4 nanoparticles were attached to the surface of MWCNT. BET surface area is 22.08 (m^2/g).

Statistical analysis

Statistical analysis by response surface methodology (RSM) was used to determine a well-fitted regression model of adsorption process. The experimental data of each adsorbate (Pb(II) and Co(II)) were fitted with linear, interactive, quadratic and cubic models to get the regression equations. The significance of suggested regression models for each adsorbate could be determined through the ANOVA. The final empirical equations obtained from experimental data which demonstrate the relationship between contaminant removal efficiency and independent variables are given in Eqs. (3) and (4) for Pb(II) and Co (II), respectively.

$$R_{Pb}\% = 87.0125 + 0.45375\times A + 0.283\times B + 0.6354\times C - 1.686\times D + 0.353\times E - 0.7707\times A^2 - 0.354\times B^2 - 0.692\times C^2 + 0.4117\times D^2 \quad (3)$$

$$R_{Co}\% = 73.96 + 0.39\times A + 0.24\times B + 0.54\times C - 1.43\times D + 0.3\times E - 0.012\times B\times C + 0.14\times C\times D - 0.66\times A^2 - 0.3\times B^2 - 0.59\times C^2 + 0.35\times D^2 \quad (4)$$

where, R_{Co} and R_{Pb} are the predicted responses for the removal efficiency of Co(II) and Pb(II) respectively, and A, B, C,D and E are the coded values of pH, time, adsorbent dosage, initial contaminant concentration and temperature, respectively. Fig. 3 shows the normal plot residuals.

Results of ANOVA for the removal of process were presented in Tables 2 and 3, respectively. The Fisher variation ratio (F-value) is a statistically valid measure of how well the factors describe the variation in the data about its mean. The regression models were statistically significant with a confidence level of 95% at an calculated F-value of 5.27 for Co(II) and 8.01 for Pb(II) with a low probability value. The Model F-value of

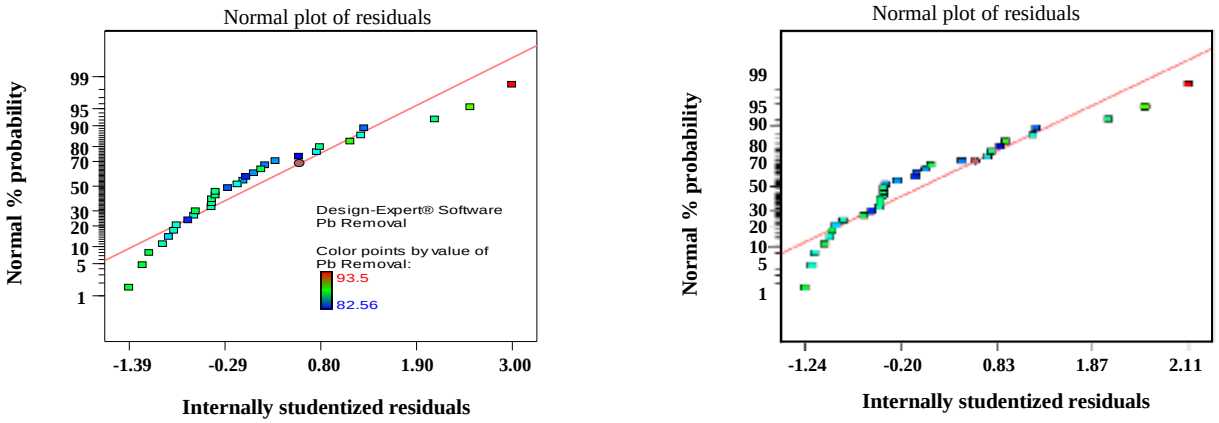

Fig. 3: Normal plot of residuals for Pb and Co. removal equations.

5.27 and 8.01 implies the models are significant. There is only a 0.05% chance that a "Model F-Value" this large could occur due to noise. Values of "Prob > F" less than 0.0500 indicate model terms are significant. Values greater than 0.1000 indicate the model terms are not significant. The "Lack of Fit F-value" of 1.32 and 1.6 implies the Lack of Fit is not significant relative to the pure error. There is a 31.76 and 38.42% chance that a "Lack of Fit F-value" this large could occur due to noise for Pb and Co respectively. Non-significant lack of fit is good -- we want the model to fit. "Adeq Precision" measures the signal to noise ratio. A ratio greater than 4 is desirable. In these models, ratio of 13.294 and 15.4 indicates an adequate signal for Pb and Co respectively. This model can be used to navigate the design space.

The value of determination coefficient (R^2) determines the goodness-of-fit of the models. The adjusted R^2 (R^2 adj) and predicted R^2 should be within approximately 0.20 of each other to be in reasonable agreement. The close correspondence between R^2 adj and R^2 indicates that unnecessary variables have not been included. The R^2 values of 0.94 and 0.86 respectively, for Pb(II) and Co(II) removal models showed the well fitness of regression models for predicting the removal results. p-Value is used to determine the effects in the model that are statistically significant. The significance of the data is determined by its p-value being closer to zero. The main effect of each factor and the interaction effects are statistically significant when p-value is less than 0.05. As can be seen from Tables 2 and 3, all the p-values of A, C and D are less than 0.05, which indicates that these variables are significant on the removal of Pb(II). Based on this hypothesis, A, B, C, D, BC and CD are the significant variables on the removal of Co(II). Response surface plots were used to determine the individual and interaction effects of the input variables on the target responses. They analyze the geometric nature of the surface, the maxima and minima of the response and the significance of the coefficients of the equation.

Cobalt removal

The response surface plots were obtained by varying two factors while keeping the other constant. Fig. 4 represents the effect of different parameters on Co(II) removal. It shows that the initial Co(II) concentration had a negative effect on the removal efficiency of Co(II) ions, in which by increasing the initial concentration of Co(II), the removal efficiency decreased.This behavior could be related to the complexity of competitive adsorption of the metal ions at different concentrations on the surface of the nanoparticles. In the higher range of adsorbate concentration, the surface of adsorbent began to get saturated and results in decreasing the adsorption efficiency of Co(II) ions. As shown in Fig. 3, solution pH was the other significant factor and showed a positive effect. The pH of the zero point of charge (pHzpc) value for nanocomposite is about 6.7. Electrostatic attraction is considered as the main adsorption mechanism at pH values higher than the pHzpc. Metal ions can also adsorb on the surface of nanocomposite through the ion exchange process at pH values less than the pHzpc (the exchange of proton with cation).The low removal efficiency of Co(II) at pH values below the pHzpc is attributed to the positively charged of the nanocomposite surface.

Table 2: ANOVA results of the regression model for optimization of Pb adsorption (determination coefficient (R2) = 0.94; adjusted determination coefficient (R2adj) = 0.90).

Response	1	Pb Removal				
ANOVA for Response Surface Quadratic Model						
Analysis of variance table [Partial sum of squares - Type III]						
	Sum of		Mean	F	p-value	
Source	Squares	df	Square	Value	Prob > F	
Model	131.2631	20	6.563153	8.011691	0.0005	significant
A-pH	4.941337	1	4.941337	6.031928	0.00319	
B-t	1.921004	1	1.921004	2.344984	0.0539	
C-D	9.690104	1	9.690104	11.82878	0.0055	
D-C0	68.24254	1	68.24254	83.30419	< 0.0001	
E-T	3.003338	1	3.003338	3.666197	0.0819	
AB	0.191406	1	0.191406	0.233651	0.6383	
AC	0.218556	1	0.218556	0.266793	0.6157	
AD	0.085556	1	0.085556	0.104439	0.7526	
AE	0.452256	1	0.452256	0.552073	0.4730	
BC	0.003306	1	0.003306	0.004036	0.9505	
BD	0.375156	1	0.375156	0.457956	0.5126	
BE	0.068906	1	0.068906	0.084114	0.7772	
CD	0.412806	1	0.412806	0.503916	0.4926	
CE	0.068906	1	0.068906	0.084114	0.7772	
DE	0.191406	1	0.191406	0.233651	0.6383	
A^2	18.30693	1	18.30693	22.34741	0.0006	
B^2	4.097546	1	4.097546	5.001906	0.0470	
C^2	14.83905	1	14.83905	18.11414	0.0014	
D^2	4.518983	1	4.518983	5.516357	0.0386	
E^2	1.568646	1	1.568646	1.914858	0.1939	
Residual	9.011167	11	0.819197			
Lack of Fit	5.531633	6	0.921939	1.324802	0.3176	not significant
Pure Error	3.479533	5	0.695907			

Table 3. ANOVA results of the regression model for optimization of Co adsorption (determination coefficient (R2) = 0.91; adjusted determination coefficient (R2adj) = 0.86).

Response	2	Co Removal				
ANOVA for Response Surface Quadratic Model						
Analysis of variance table [Partial sum of squares - Type III]						
	Sum of		Mean	F	p-value	
Source	Squares	df	Square	Value	Prob > F	
Model	94.83756	20	4.741878	5.278807	0.000428	significant
A-pH	3.570116	1	3.570116	3.974365	0.027321	
B-t	1.387926	1	1.387926	1.545082	0.043181	
C-D	7.0011	1	7.0011	7.793844	0.00471	
D-C0	49.30523	1	49.30523	54.88813	< 0.0001	< 0.0001
E-T	2.169911	1	2.169911	2.415613	0.090144	
AB	0.138291	1	0.138291	0.15395	0.546675	
AC	0.157907	1	0.157907	0.175787	0.527319	
AD	0.061814	1	0.061814	0.068814	0.644568	
AE	0.326755	1	0.326755	0.363754	0.405103	
BC	0.002389	1	0.002389	0.002659	0.041406	
BD	0.27105	1	0.27105	0.301742	0.439019	
BE	0.049785	1	0.049785	0.055422	0.665636	
CD	0.298253	1	0.298253	0.332024	0.047042	
CE	0.049785	1	0.049785	0.055422	0.665636	
DE	0.138291	1	0.138291	0.15395	0.546675	
A^2	13.22676	1	13.22676	14.72444	0.000514	
B^2	2.960477	1	2.960477	3.295696	0.040253	
C^2	10.72121	1	10.72121	11.93519	0.001199	
D^2	3.264965	1	3.264965	3.634662	0.033059	
E^2	1.133347	1	1.133347	1.261677	0.166067	
Residual	6.510568	11	0.59187			
Lack of Fit	3.996605	6	0.666101	1.640212	0.3842	not significant
Pure Error	2.513963	5	0.502793			

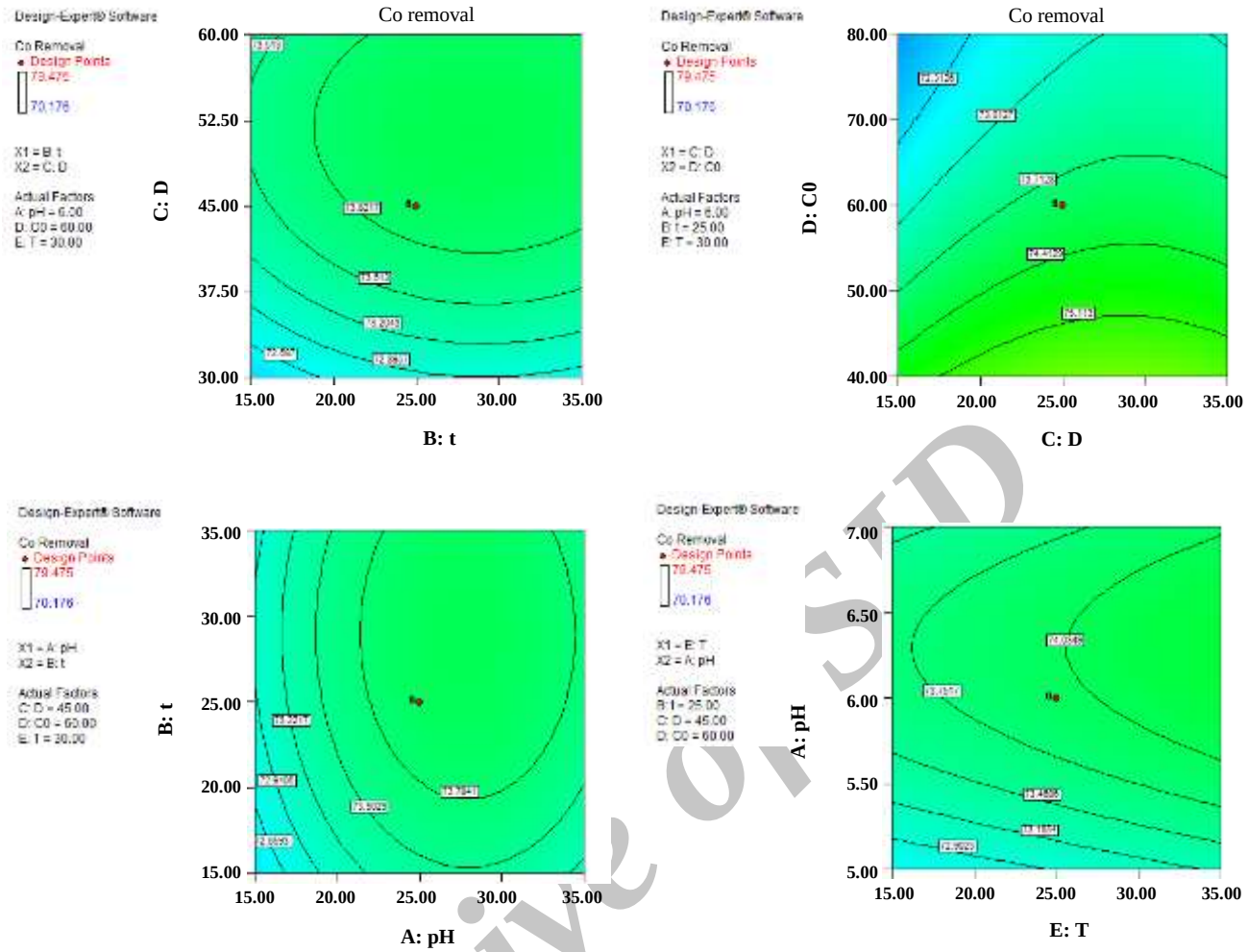

Fig. 4 RSM plot for Co(II) removal

The removal of Co(II) at the pH values lower than the pHzpc, is justified by the exchange of adsorbed proton with Co(II) ions. As shown in Fig. 4, solution sorbent dosage was the other significant factor and showed a positive effect. The increasing of removal percentage with sorbent dosage is because of the availability of more adsorption and exchange sites for metal ions and then by overlapping of active sites, equilibrium was established between the sorbent and the metal ions. Contact time and solution temperature are the next factors which have little effect on process removal efficiency. Increasing temperature too much, had a relatively significant positive effect on the removal efficiency of Co(II) ions. The increased removal of Co (II) ions with increasing temperature may be a result of the faster chemical precipitation rate of lead hydroxide at the higher temperatures. Although the increase in each of time and adsorbent dosage parameters individually had a positive effect on the removal efficiency of Co(II) ions, the simultaneous increase of these parameters showed a negative synergistic effect on the removal. The simultaneous increase of initial concentration and dosage parameters showed a positive synergistic effect on the removal.

Figs. 5 show the effects of significant variables on the removal efficiency of Pb(II) ions. The removal efficiency of Pb(II) on nanocomposite was very sensitive to the changes in solution pH . It shows that increasing in pH value from 4 to7 resulted in enhancing the removal efficiency of Pb(II) ions from 81.29% to 90.47%.

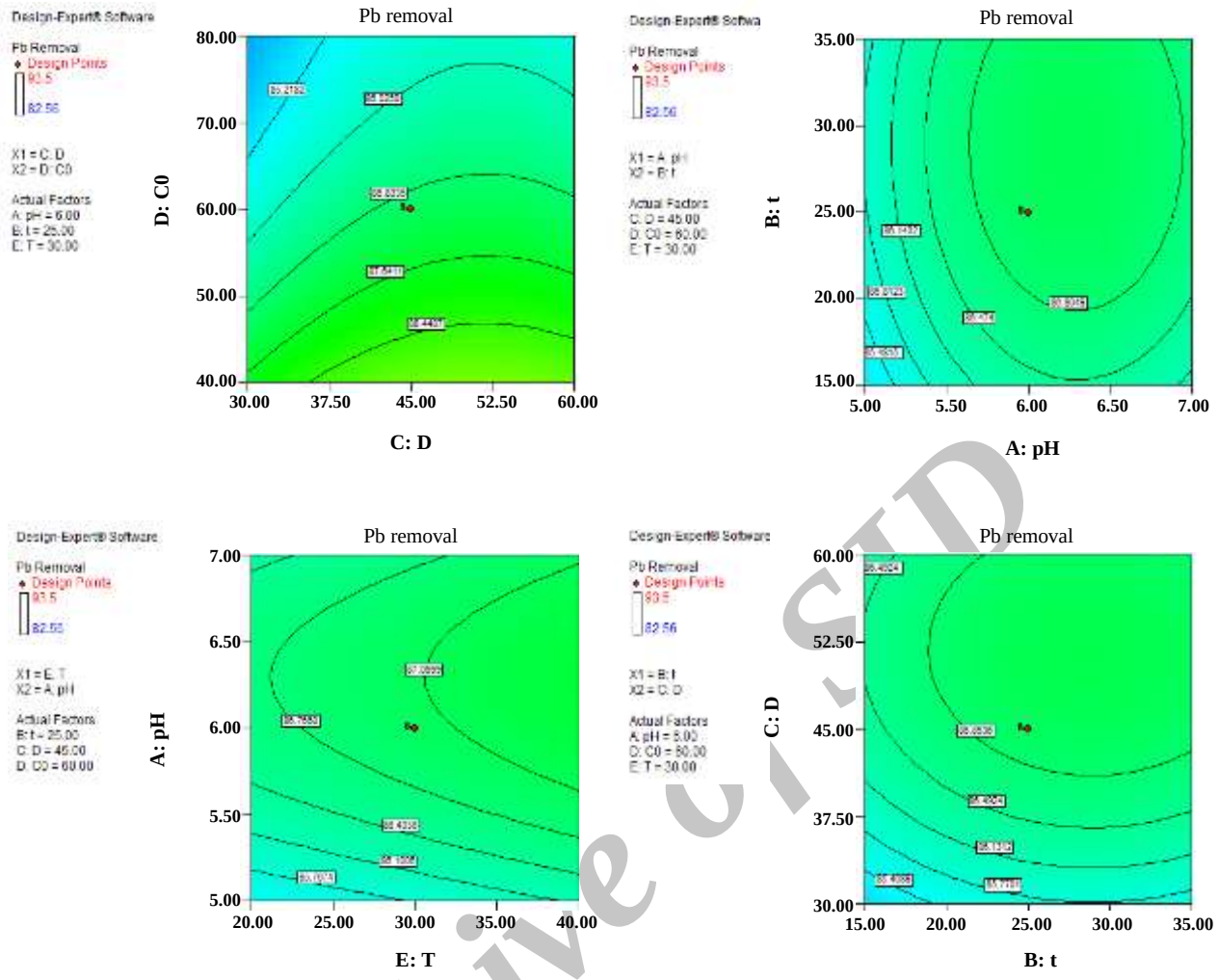

Fig. 5: RSM plot for Pb(II) removal.

It can also be pointed out that at the pH values lower than the pHzpc, some Pb(II) ions can be adsorbed on the surface of nanocomposite nanoparticles through the ion exchange process. It was reported that the precipitation of lead hydroxide can play a leading role during heavy metal removal process at pH above 6. The effect of temperature and pH on the removal efficiency of Pb(II) ions is represented in Fig. 5. The interactive effects of initial concentration and adsorbent dosage were shown in Fig. 4. They show that increasing in adsorbent dosage has the highest effect on the adsorption of Pb(II) ions. This behavior could be ascribed to a greater surface area and the more availability of adsorption sites at the higher adsorbent dosage.

Optimization

Maximum removal efficiency for each adsorbate and the corresponding optimal conditions of variables were determined and the models were confirmed by some further experimental runs. Numerical optimization was done to find a maximum point for the desirability function by setting the values of pH, time, temperature, concentration of initial ions and adsorbent dosage within their ranges and maximizing the removal efficiencies of Co(II) and Pb(II) ions. As can be seen in Fig. 6, the best local maximum value was found to be at the initial solution pH of 6.58, the temperature of 40 °C, the initial ion concentration of 35 mg/L, contact time of 25.3 min and the adsorbent (dosage of 48.3 mg/50L). In this condition the removal efficiencies of Co(II) and Pb(II)

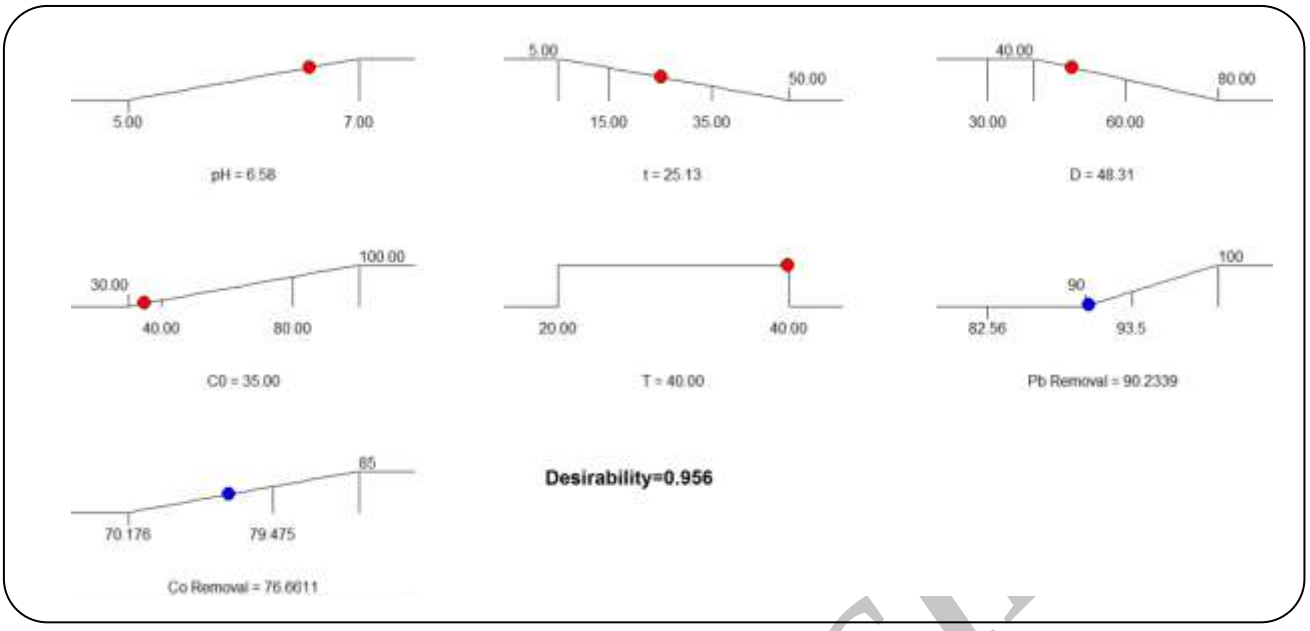

Fig. 6: Optimization results obtained by RSM.

ions were 79.4%, and 90.2%, respectively and the desirability value was found to be 0.956. This optimum condition was checked experimentally. The results showed the removal efficiency of 75.4%, 98.4% and Co(II) and Pb(II) ions, respectively. The high degree of agreement between the predicted optimum conditions and the repeated experimental results indicated that the central composite Design could be employed as an effective and reliable tool for evaluation and optimization of the effects of adsorption parameters on the removal efficiency of heavy metals using Fe3O4-MWCNT nanocomposite.

The absorption amount increase with increasing pH. This is due to the surface complexation reactions, which are mostly influenced by the electrostatic force of attraction between copper and the surface of the adsorbent. The removal of metals can be derived into two stages: one in which the removal rate is very high, followed by a second stage with a much lower removal rate. The rapid removal of the adsorbate has significant practical importance as it will facilitate smaller reactor volumes ensuring efficiency and economy. In the case of absorbent dosage, when the adsorbent dosage is higher, there is a very fast adsorption onto the adsorbent surface, which results in a lower adsorbate concentration in the solution. However, the adsorption sites on the adsorbent surface remain unsaturated when the adsorbate concentration in the solution drops to a lower value.

Comparing the absorbent with literature

The results of removal efficiency in optimized condition were compared by the absorbent presented in the literature (Table 4). The results showed that the synthesized absorbent has a better performance than the presented absorbents.

Kinetic and Isotherm models

For the solid-liquid system, the studies of adsorption isotherms are very important to realize information about adsorption capacity of adsorbents. The widely used isotherm equations for evaluating the adsorption equilibrium are Langmuir , Freundlich isotherms and Dubinin-Radushkevich isotherm. Correlation coefficient (R2) shows that the Langmuir model is better than the other models in simulation of the adsorption isotherm. The agreement of the Langmuir model with the experimental results suggests that a monolayer coverage of metals on the outer surface of the adsorbent.

There are essentially three steps in the adsorption process by porous adsorbents [34]: (1) solute transfer from the bulk solution to the external surface of the adsorbent through a liquid boundary layer (liquid film diffusion), (2) solute transfer from the adsorbent surface to the intraparticle active sites (intraparticle diffusion), and (3) interactions of the solute with the available sites on both the external and internal surfaces of the adsorbent (chemical reaction). One or more of the above-mentioned

Table 4: Synthesized absorbent comparison with the literature[17].

Co	Pb	Absorbent
-	97.1%	γ-Fe_2O_3
56.1%	93.1%	Thiosalicylhydrazide-Modified Magnetic Nanoparticles
-	86%	MWCNT
-	93.1%	nano mesoporous silica
-	95%	nano scale zero valent iron
75.8%	-	Ethyl acrylate grafted chitosan
83%	-	natural lignite

Table 5: Isotherm models parameters.

Adsorbed metal	Temperature	Langmuir isotherm			
		q_m(mg/g)	K_L(L/mg)	R_L	R^2
Pb (II)	25°C	68.83	0.0371	0.063	0.986
Co (II)	25°C	67.47	0.0280	0.082	0.990
		Freundlich isotherm			
		K_F(mg/g)	n		R^2
Pb (II)	25°C	15.95	4.062		0.909
Co (II)	25°C	12.31	3.531		0.942
		Dubinin-Radushkevich isotherm			
		q_{DR}(mmol/g)	B_{DR}(mol^2/J^2)*10^8	E(KJ/mol)	R^2
Pb (II)	25°C	0.984	6.349	2.806	0.972
Co (II)	25°C	1.076	9.092	2.345	0.953

steps may control the rate at which the solute is adsorbed and the amount of solute that is adsorbed onto the adsorbents. To identify the step governing the overall removal rate of the adsorption process, Pseudo First order. Pseudo second order and Morris-Webber models were applied. The agreement of the Pseudo second order model with the experimental results suggests that liquid film diffusion, intraparticle diffusion, and chemical reaction are controlling mechanism.

CONCLUSIONS

In this research, Fe3O4-MWCNT nanocomposite were synthesized and used to remove some heavy metal ions, i.e. Co(II) and Pb(II), from aqueous solutions. Response surface methodology was used to find a maximum location in the design space. A central composite Design was employed to evaluate the effects of pH, time, temperature, initial contaminant concentration and adsorbent dosage on the removal efficiency of metal ions on Fe_3O_4-MWCNT nanocomposite under competitive conditions. Quadratic models were well fitted to the experimental data and second-order polynomial equations (regression models) were described the relationship between the responses and the variables accurately. Results showed that the initial concentration of Pb(II), adsorbent dosage and pH were the most significant parameters on the removal efficiency of Pb(II) ions. pH, time, Adsorbent dosage and initial concentration and their interaction effects had the most significant influences on the removal efficiency of Co(II) ions. The corresponding optimal conditions of variables of adsorption process were determined to be at the pH of 6.58, the temperature of 40 °C, contact time of 25.3 min , the initial metal concentration of 35 mg/L

(each metal ion) and the adsorbent dosage of 48.3 mg/50L. In this condition the removal efficiencies of Co(II) and Pb(II) ions were 79.4%, and 90.2%, respectively and the desirability value was found to be 0.956. The equilibrium data were well fitted by the Langmuir model. The removal mechanism of metal ions followed adsorption and ion exchange processes.

Received : Sep. 28, 2016 ; Accepted : Nov. 13, 2017

REFERENCES

[1] Fenglian F.u., Qi W., Removal of Heavy Metal Ions From Wastewaters: A Review, *Journal of Environmental Management*, **92**(3):65-81 (2011).

[2] Barakat M.A., New Trends in Removing Heavy Metals From Industrial Wastewater, *Arabian Journal of Chemistry*, **4**(4):361–377 (2011).

[3] Lim A.P., Aris A.H., A Review on Economically Adsorbents on Heavy Metals Removal in Water and Wastewater, *Reviews in Environmental Science and Bio/Technology*, **13**(2):163-181 (2014).

[4] Solat Sana, Reza Roostaazad, Soheila Yaghmaei, Biosorption of Uranium (VI) from Aqueous Solution by Pretreated Aspergillus Niger Using Sodium Hydroxide, *Iran. J. Chem. Chem. Eng.(IJCCE)* **34**(1):65-74 (2015).

[5] Marziyeh Sanchooli Moghaddam, Somayeh Rahdar, Mahmoud Taghavi, Cadmium Removal from Aqueous Solutions Using Saxaul Tree Ash, *Iran. J. Chem. Chem. Eng.(IJCCE)*, **35**(3):45-52 (2016).

[6] Bhatti Haq Nawaz, Khadim Rubina, Hanif Muhammad Asif, Biosorption of Pb(II) and Co(II) on Red Rose Waste Biomass, *Iran. J. Chem. Chem. Eng.(IJCCE)*, **30(**4):81-87 (2011).

[7] Xiao-fei T., et al., Biochar-based Nano-Composites for the Decontamination of Wastewater: A Review Bioresource Technology, *Bioresource Technology*, **212**:318–333 (2016).

[8] Ghasemi, Z., H. Younesi, A. Akbar Zinatizadeh, Kinetics and Thermodynamics of Photocatalytic Degradation of Organic Pollutants in Petroleum Refinery Wastewater over Nano-TiO_2 Supported on Fe-ZSM-5, *Journal of the Taiwan Institute of Chemical Engineers*, **65**:357–366 (2016).

[9] Liwei F., Zhang S., Zhang X., Zhou H., Lub Z., Wang S., Removal of Arsenic from Simulation Wastewater Using Nano-Iron/Oyster Shell Composites, *Journal of Environmental Management*, **156(**1):109–114 (2015).

[10] Chen H., Luo H.J., Lan Y.C., Dong T.T., Hu B.J., Wang Y.P., Removal of Tetracycline From Aqueous Solutions Using Polyvinylpyrrolidone (PVP-K30) Modified Nanoscale Zero Valent Iron, *J. Hazard. Mater*, **92**:44-53 (2011).

[11] Khan N.A., Khan K.A., Islam M., "Water and Wastewater Treatment using Nano-technology" Chemistry of Phytopotentials: Health, Energy and Environmental Perspectives , Springer Berlin Heidelberg Section C , 315-318 (2012).

[12] Ming H., Shujuan Z., Bingcai P., Heavy Metal Removal From Water/Wastewater by Nanosized Metal Oxides: A Review, *Journal of Hazardous Materials*, **211–212**(15):317–331 (2012).

[13] Byung Hyo K., Michael J. H., Jongnam Park, Synthesis, Characterization, and Application of Ultrasmall Nanoparticles, *Chem. Mater*, **26**(1):59–71 (2014).

[14] Mandavian A.R., Mirrahimi M.A.S., Efficient Separation of Heavy Metal Cations by Anchoring Polyacrylic Acid on Superparamagnetic Magnetite Nanoparticles Through Surface Modification, *Chem. Eng. J*, **159**:264–271 (2010).

[15] Chen Y.H., Li F.A., Kinetic Study on Removal of Copper (II) Using Goethite and Hematite Nano-Photocatalysts, *J. Colloid Interface Sci*, **347**:277–281 (2010).

[16] Badruddoz A.Z.M., Tay A.S.H., Tan P.Y., Hidajat K., Uddin M.S., Carboxymethyl-beta-cyclodextrin Conjugated Magnetic Nanoparticles as Nano-Adsorbents for Removal of Copper Ions: Synthesis and Adsorption Studies, *J. Hazard. Mater*, **185**:1177–1186 (2011).

[17] Ihsanullaha A., Adnan M. A., Tahar L., Heavy Metal Removal from Aqueous Solution by Advanced Carbon Nanotubes: Critical Review of Adsorption Applications. *Separation and Purification Technology*, **157(**8):141–161 (2016).

[18] Wang H., Yan N., Li Y., Zhou X.H., Chen J., Yu B.X., Gong M., Chen Q.W., Fe Nanoparticle-Functionalized Multi-Walled Carbon Nanotubes: One-Pot Synthesis and Their Applications in Magnetic Removal of Heavy Metal Ions, *J. Mater. Chem*, **22:** 9230- 9236 (2012).

[19] Jun X.U.Y., Arrigo R., Xi L.I.U., Sheng S.D., Characterization and Use of Functionalized Carbon Nanotubes for the Adsorption of Heavy Metal Anions, *New Carbon Mater*, **26**:57-62 (2011).

[20] Khaldi F.A.A., Sharkh B.A., Abulkibash A.M., Atieh M.A., Cadmium Removal by Activated Carbon, Carbon Nanotubes, Carbon Nanofibers, and Carbon Fly ash: A Comparative Study, *Desalin. Water Treat*, **53**:1417–1429 (2015).

[21] Hadavifar M., Bahramifar N., Younesi H., Li Q., Adsorption of Mercury ions from Synthetic and Real Wastewater Aqueous Solution by Functionalized Multi-Walled Carbon Nanotube with Both Amino and Thiolated Groups, *Chem. Eng. J*, **237:**217–228 (2014).

[22] Moghaddam H.K., Pakizeh M., Experimental Study on Mercury Ions Removal From Aqueous Solution by MnO_2/CNTs Nanocomposite Adsorbent, *J. Indus. Eng. Chem*, **21:**221–229 (2015).